Performance of Simulcast Wireless Techniques for Personal Communication Systems

Sirikiat Ariyavisitakul, *Senior Member, IEEE*, Thomas E. Darcie, *Senior Member, IEEE*, Larry J. Greenstein, *Fellow, IEEE*, Mary R. Phillips, *Member, IEEE*, and N. K. Shankaranarayanan, *Member, IEEE*

***Abstract*—Broadband analog transport facilities using fiber or fiber/coax cable can play a significant role in the evolution of the network infrastructure for personal communications services (PCS's). Low-power PCS systems require a dense grid of radio ports to provide connectivity to the telephone network. Analog transport has a number of important advantages over digital transmission facilities, including the flexibility to support a variety of air interface formats, shared infrastructure cost with other services such as video distribution, and centralized call processing allowing the use of low cost and simple radio ports. A simulcast technique can be used in such systems to permit low rates of handoff (no handoff within each simulcast area) and sharing of hardware resources among multiple radio ports.**

This paper provides a detailed model and a simulation analysis of the cochannel interference and noise performance as well as the resource sharing benefit of a simulcast PCS system. Several potential PCS air interfaces are considered, including time division multiple access (TDMA) and code division multiple access (CDMA) techniques. Our investigation shows that the impact of multiple antenna noise in a simulcast system is offset by the improved signal-to-interference (SIR) ratio brought about by distributed antennas. Even with distributed antennas, multiple antenna noise places a limit on the maximum number of radio ports that can be assigned to each simulcast group. This limit, however, is shown to have little impact on the achievable resource sharing benefit of simulcasting (i.e., grouping beyond this limit has diminishing returns). A saving of 40% to 60%, in terms of the required central hardware resources, is typical for both TDMA and CDMA systems in suburban environments.

I. Introduction

Interest in personal communications services (PCS) has grown rapidly over the last decade. In 1993, the FCC announced rules for PCS spectrum allocation which allow for a variety of competing networks and services [1]. Evolving microcellular and wireless loop access architectures emphasize the use of low power radio technology to achieve high capacity through massive frequency reuse, and to reduce power consumption of the PCS handsets. Low-power PCS systems will require a dense grid of fixed radio ports and a large transport infrastructure to provide connectivity to the telephone network.

Broadband transmission facilities using analog fiber or fiber/coax cable can play a significant role in the evolution of the network infrastructure for public PCS access [2]–[9]. Analog transport over a broadband network permits radio ports to be low cost and simple, since all per-call processing circuits of the system are located in the central location. Furthermore, the infrastructure cost for analog backhauling is minimized if the transport network is shared with other services such as video distribution. Analog transport also adds a degree of flexibility in the provisioning of radio ports. A simulcast arrangement can be used to achieve resource sharing advantages among different radio ports. The simulcast approach considered in this study has the following attributes [10]:

1) *Grouping*: In low-traffic or low-penetration service areas, multiple radio ports can be grouped to form a larger set of radio users that share common cable spectrum and call processing hardware resources.
2) *Simulcasting*: The radio signals are simulcast from all the radio ports within each group, so there is no handoff when a user moves between two microcells within the same simulcast group (a "microcell" is the coverage area of each radio port). A similar concept is known as "distributed antennas," as denoted in [11]–[15].
3) *Dynamic Load Balancing*: The grouping of radio ports can be rearranged according to traffic load variations. For example, traffic "hot spots" can be accommodated by assigning all the resources of a group server to a fewer number of radio ports. This can be done in a dynamic manner at the central hub without modifying the transport infrastructure.

As the size of a (micro)cell becomes smaller in low-power PCS systems, the variation in traffic demand at each microcell is expected to become larger. Without simulcasting, spectrum and hardware resources must be budgeted for some maximum traffic at each cell even though the *average* traffic density over the entire service area is quite low, e.g., in suburban environments.

This paper provides a detailed performance model and a simulation analysis of a simulcast PCS system. The principle of simulcasting and distributed antennas is not new. However, we present new results on the quantitative performance of such systems, for different PCS air interfaces, taking into account both cochannel interference and thermal noise as well as traffic statistics and propagation into buildings. Section II provides the overall system concept. Section III describes the radio propagation model for suburban PCS systems. We focus on the suburban environment because this is where resource

Manuscript revised December 1995.

S. Ariyavisitakul, T. E. Darcie, L. J. Greenstein, and N. K. Shankaranarayanan are with AT&T Research, Holmdel, NJ 07733 USA.

M. R. Phillips is with ATx Telecom Systems, Naperville, IL 60563 USA.

Publisher Item Identifier S 0733-8716(96)01948-8.

0733–8716/96$05.00 © 1996 IEEE

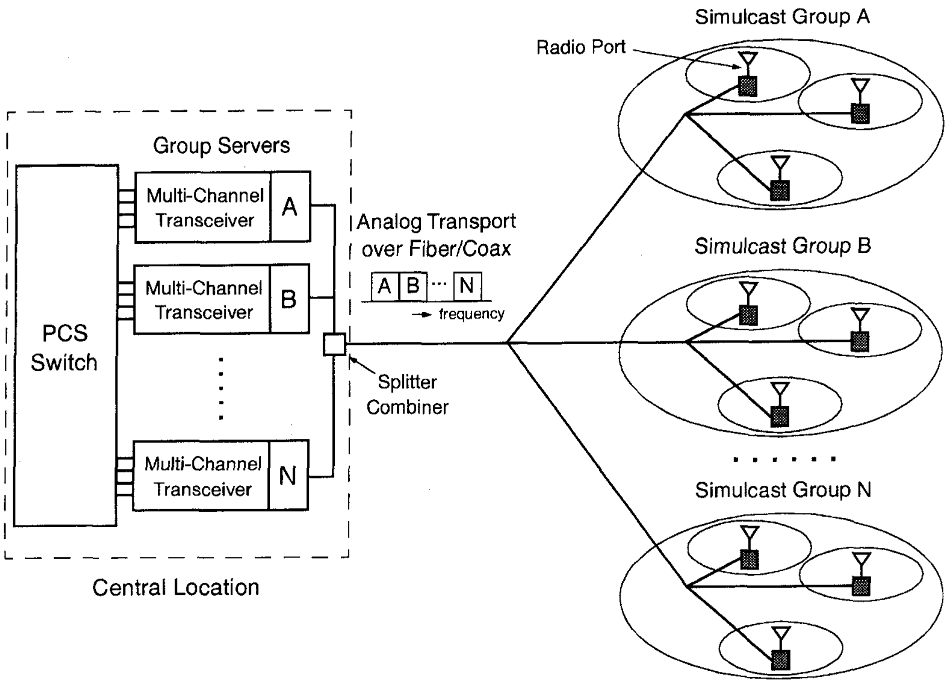

Fig. 1. A simulcast PCS system.

sharing is critically needed. Section IV provides details of the air interface models; different potential PCS wireless technologies are considered, including time division multiple access (TDMA) and code division multiple access (CDMA) techniques. Section V presents link budget analyses for these wireless techniques. The link budget is used to determine the maximum allowed coverage area size of each radio port, which is a crucial parameter in assessing the resource sharing benefit of simulcasting. Section VI describes the simulcast arrangement for each of the wireless techniques considered—it presents simulation results that demonstrate the cochannel interference and thermal noise performance as well as the resource sharing advantage of the system as a function of the number of microcells assigned to each simulcast group.

II. System Architecture

Figure 1 depicts the concept of a simulcast PCS system. The system uses analog transport broadband network to carry RF signals between radio ports and a central location. The radio port contains only analog circuits such as a transmit linear amplifier, a receive low-noise amplifier, and a frequency converting filter which performs radio-RF/transport-RF frequency translation. All per-user functions are located at the central location. Each multichannel transceiver serves a group of radio ports via an analog, frequency-division multiplex (FDM) interface on the transport network. For example, in Fig. 1, server A uses frequency subband A over fiber/coax to serve radio ports in simulcast group A. The downstream signal from each server is received by all the radio ports in its serving group. The radio ports in the same group then simulcast the information using either the same air frequency for all ports (i.e., distributed antennas) or different frequencies for different ports depending on the air interface protocol, to be discussed later. In the upstream direction, the radio signals from different radio ports in the same group share the same analog transport medium. These signals are summed with random phase over the transport network, giving rise to increased thermal noise, referred to as "multiple antenna noise." By making the frequency oscillators in the radio ports programmable, the assignment of radio ports to group servers can be changed dynamically as traffic dictates.

III. Radio Propagation Model

Much work has been done to characterize radio propagation in and around buildings and houses in suburban environments [16]–[23]. Measurements indicate significant variations in the radio propagation characteristics at different user locations within the desired coverage area. The suburban propagation model used in this study is based on measurement results at 815 MHz given in [18, Fig. 26]. The following median path loss formula was obtained from a linear regression of the measured mean signal levels (where the averaging is over a small local area) at various locations inside and outside eight suburban houses using a 8.2-m high outdoor port antenna:

$$L(d)_{\mathrm{dB}} = 45 \log d(m) - 3.8. \tag{1}$$

The median path loss $L(d)$ increases as $d^{4.5}$, where d is the propagation distance. The standard deviation σ of the log normal variation around the regression line is 10 dB. This variation is commonly referred to as shadow fading.

In order to use the above results for systems in the new bands [1], we need to scale the 815 MHz path loss to 2 GHz. Considering the frequency-squared difference due to antenna aperture, the path loss at 2 GHz would be 7.8 dB higher than at 815 MHz (the square of the ratio of the two frequencies), yielding[1]

$$\text{Suburban Residential}: L(d)_{\text{dB}} = 45 \log d(m) + 4.0. \quad (2)$$

It should be noted that this model, when compared with outdoor models such as Hata's [24], or the double regression model [25], yields higher median path loss. This is because we take transmission loss through walls into account for communications to users inside buildings. This leads to smaller cell sizes, even when using air interfaces designed for high tier cellular services (see Section V).

Shadow fading in microcellular environments has been modeled as the sum of two independent log-normal components [26]: a user-location specific component, and a path-specific component. The user-location specific component is the same for all radio paths to or from a given user; this accounts for the effect of building attenuation, i.e., the signals are affected by walls equally in all directions. The path-specific components are distinct and independent for all radio paths. Similar to earlier studies [15], [27], we assume that the user-location specific component has a standard deviation $\sigma_L = 6$ dB, and the path-specific component has a standard deviation $\sigma_P = 8$ dB. This gives $\sigma = \sqrt{\sigma_L^2 + \sigma_P^2} = 10$ dB. This model will be used in later performance analyses.

IV. Air Interfaces

The simulcast PCS system uses analog transport, which permits a wide range of air interface formats to be supported over the same infrastructure. Recent FCC rules [1] allocated 120 MHz of spectrum near 2 GHz for licensed PCS access. The licensed spectrum included 30 MHz bands and 10 MHz bands which were partitioned in a split band fashion to allow frequency-division duplex (FDD) operation. Several different wireless technologies are currently being considered for the PCS common-air standard [28]. It is also possible that multiple common-air standards will be adopted.

Table I summarizes air interface details of the potential PCS wireless technologies to be considered in this study. A 10 MHz allocation using FDD is assumed for all systems. The TDMA techniques include Bellcore PACS (similar to UDPC or WACS [29]–[31]) and two other TDMA proposals, upbanded IS-54 and DCS-1900, which are upbanded versions (from 900 MHz to 2 GHz) of the existing digital cellular standards IS-54 and GSM [32]–[34], respectively. The CDMA system, IS-95*, is a fictitious air interface proposal. It is similar to the existing CDMA cellular standard IS-95 [35], [36] (which also has a PCS proposal version [37]) except for a few straightforward changes to improve the speech quality up to the wireline standard[2] and to make the signal span the entire 5 MHz available bandwidth on each FDD channel. These changes include scaling up the chip rate and speech rate by a factor of four, and the use of standard, adaptive differential pulse code modulation (ADPCM) [38] instead of the IS-95 lower rate speech coding (IS-96). These straightforward changes may have impact on the estimated system capacity compared to a more efficient implementation alternative. The purpose of this study is not to make a one-to-one comparison of different air interface techniques, but rather to show how the simulcast concept can be applied to existing wireless technologies.

The conditions for the minimum required signal-to-interference-plus-noise ratio (SINR) in Table I merit some discussion. First of all, the signal and interference powers in this ratio are the averages over their Rayleigh fadings, i.e., local spatial averages of these powers. For PACS, an SINR of 16 dB is required to achieve a specified frame-error rate between 2% and 3% in quasistationary Rayleigh fading with two-branch antenna selection diversity. The required SINR's for upbanded IS-54, DCS-1900, and IS-95* in Table I are based on values reported for their cellular standard versions. Cellular IS-54 uses antenna diversity on the uplink but not the downlink, so, as Table I shows, the required SINR is smaller for the uplink than for the downlink. GSM (or "cellular" DCS-1900) does not include antenna diversity, but relies on the use of slow frequency hopping and channel coding/interleaving to combat Rayleigh fading. These required SINR's may not directly apply to PCS environments but can be invoked for our purposes nonetheless. This is because it is most likely that each system would be modified in some way, as necessary, to provide the requisite performance quality in PCS environments for similar SINR's. Since it is not our purpose to re-engineer the details of the air interface techniques, we simply make the *ad hoc* assumption here that the required SINR's in Table I are applicable to PCS environments for all the systems.

V. Coverage Area Design

A. Coverage Objective

This section derives, for the different air interfaces, the maximum allowable microcell sizes for specified coverage objectives. We do this first for the *non*simulcast situation. In simulcast situations, uplink noise power increases because of multiple antennas, but at the same time cochannel interference can be reduced. These issues are discussed in Section VI. We will show there the conditions under which the coverage objectives are met or exceeded using the microcell sizes derived here.

A reasonable objective of coverage area design in PCS's is to provide adequate radio link quality in as high as 99% of all user locations. The link quality threshold is given in terms of the minimum required SINR, so both the signal-to-noise ratio (SNR) performance and signal-to-interference ratio (SIR) performance of the system need to be studied. Note that $\text{SINR}^{-1} = \text{SNR}^{-1} + \text{SIR}^{-1}$. Like any cellular system, the reliability of a PCS system will be limited by the existence of areas with unacceptably high path loss/shadowing (inadequate SNR) as well as areas of unacceptably high

[1] More recent measurements [23] indicated an additional path loss at 2 GHz of as much as 15 dB (instead of 7.8 dB) compared to the path loss at 815 MHz. This was reported to be the effect of foliage and increased scattering and diffraction loss at higher radio frequencies. Increased path loss would result in smaller radio port coverage areas, making the resource sharing benefit of simulcasting more significant (see Section VI).

[2] Upgraded speech quality options have not been provided for upbanded IS-54 and DCS-1900.

TABLE I
PCS WIRELESS TECHNOLOGIES

	TDMA			CDMA
	PACS	Upbanded IS-54	DCS-1900	IS-95*
Modulation	π/4 QPSK	π/4 QPSK	GMSK	QPSK
Demodulation	Coherent	Coherent	Coherent	Noncoherent (Uplink) Coherent (Downlink)
RF Channel Spacing	300 kHz	30 kHz	200 kHz	5 MHz
Noise Bandwidth	240 kHz	24 KHz	200 kHz	4.9 MHz
Channel Bit Rate (kb/s)	400	48.6	270.833	38.4
TDMA Channels/Carrier	8	3	8	N/A
Speech Coding	ADPCM	VSELP[34]	RPE-LP[34]	ADPCM
Speech Rate (kb/s)	32	7.95	13	32 (Full Rate)
Speech Activity Factor	1.0	1.0	1.0	0.5
Channel Coding[a] a. CRC: cyclic redundant check	CRC only	1/2 rate convolutional and CRC	1/2 rate convolutional and CRC	1/3 rate convolutional (Uplink) 1/2 rate convolutional (Downlink) CRC
Equalization	No	Yes	Yes	N/A
Slow Frequency Hopping	No	No	Yes	N/A
Minimum Required SINR Uplink/Downlink (dB)	16/16[31]	12/16[33]	10/10[33]	–14/–16[35][36] (before despreading)

cochannel interference (inadequate SIR). The outage produced by path loss variations can be controlled through careful link budget considerations. The SIR performance is determined by the frequency reuse factor (for TDMA) or the offered traffic density (for CDMA) of the system.

Link budget calculation is used to determine the maximum coverage area size of each radio port. The uplink usually limits the area, although power limitations can be critical on the downlink as well, especially in microcells. The remainder of this section first describes the conventional design approach and points out its limitations. We then proceed to derive simulation results which give accurate estimates of the allowed coverage area sizes for specific air interfaces.

B. Conventional Method

Define the median SNR for a user located in the corner of a polygon port coverage area as

$$\Lambda(r) = \frac{P_T G_A}{P_N L(r)} \tag{3}$$

where $L(r)$ is the median path loss, r is the distance from center to corner of a microcell (microcell radius), and P_T, P_N, and G_A are link parameters: P_T is the transmit power, P_N is the received noise power, and G_A is the combined transmit–receive antenna gain. A commonly used link budget equation is (e.g., [39])

$$\Lambda(r_{\max})_{\text{dB}} = \lambda_{0\,\text{dB}} + M_{\text{dB}} \tag{4}$$

where $r_{\max}$ is the maximum allowed microcell radius, λ_0 is the target SNR, and M is the shadow loss margin that permits 99% coverage in the absence of cochannel interference. The above link-budget equation is a convenient tool in the sense that, given a propagation model and the desired reliability, M is virtually the same for all systems (typically, around 9 dB for the suburban propagation model assumed here). The choice of λ_0, however, has not been well defined, and the implication that λ_0 can be chosen independently of SIR performance is misleading. To see why, assume that the value of SIR exceeded at 99% of all locations (denoted by $\text{SIR}_{99\%}$) is known. Choosing the target SNR λ_0 such that

$$\lambda_0^{-1} = \gamma^{-1} - \text{SIR}_{99\%}^{-1} \tag{5}$$

where γ is the desired 99% value of SINR, would not guarantee $\text{SINR} \geq \gamma$ at 99% of all locations. For, although $\text{SINR}^{-1} = \text{SNR}^{-1} + \text{SIR}^{-1}$ is true, $\text{SINR}_{99\%}^{-1} = \text{SNR}_{99\%}^{-1} + \text{SIR}_{99\%}^{-1}$ can be true only if the interference power I is a fixed parameter. But because both the signal power S and I are random variables, $\text{SINR}_{99\%}^{-1}$ can be either greater or smaller than $\text{SNR}_{99\%}^{-1} + \text{SIR}_{99\%}^{-1}$ depending on the probability density functions (pdf) of S and I. In general, finding λ_0 to satisfy

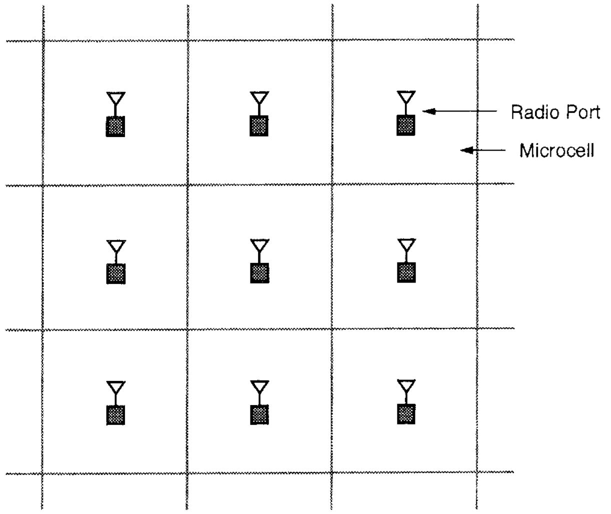

Fig. 2. Cell geometry.

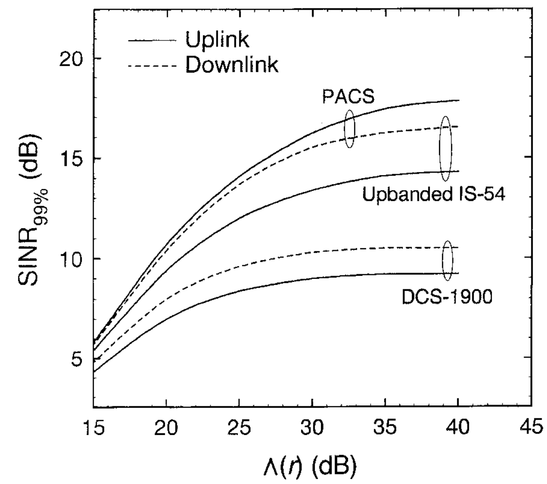

Fig. 3. $\mathrm{SINR}_{99\%}$ versus median SNR at cell corner $\Lambda(r)$ for TDMA systems. $N = 16$ for PACS and upbanded IS-54, and $N = 9$ for DCS-1900.

$\mathrm{SINR}_{99\%} = \gamma$ requires exact knowledge of the pdf's of S and I, and in most cases, since these pdf's cannot be given or approximated in an analytical form as a function of λ_0, it is impossible to solve for λ_0. We proceeded, instead, to derive simulation results which give the statistics of SINR as a function of $\Lambda(r)$.

C. Simulation Approach and Results

The simulation approach we used directly determines the minimum required values of $\Lambda(r)$ for different wireless systems. The simulations simultaneously consider many system variables and give statistics of SINR for users uniformly located throughout each port coverage area. Square coverage areas and a square grid of radio ports are assumed (see Fig. 2). There is little difference in performance between different cell geometries [40], [41]. A cell wrapping technique is used to avoid edge effects. User traffic in each microcell is generated based on an Erlang B blocked-calls-cleared model [42]. Median path losses and shadow fading are simulated according to the suburban propagation model described in Section III. Measurement-based port selection is assumed, i.e., each user accesses the port with the maximum instantaneous downlink SINR. This provides a form of macroscopic diversity against path specific shadowing (the user-location specific component is correlated for signals from all ports) and thus gives better coverage performance than distance-based port selection.

Figure 3 shows $\mathrm{SINR}_{99\%}$ as a function of $\Lambda(r)$ for different TDMA systems. The frequency reuse factor N for each system has been determined such that the achieved $\mathrm{SINR}_{99\%}$ is greater than or roughly equal to the minimum required SINR specified in Table I at high SNR, i.e., high values of $\Lambda(r)$. Only the first interfering tier is considered. $N = 16$ is adequate for PACS and upbanded IS-54. For DCS-1900, simulation results were obtained for $N = 9$. This reuse factor does not quite satisfy the minimum required SINR of 10 dB on the uplink, but the results would be better if the interference averaging effect of frequency hopping [43] were taken into account. Also, the reuse factor N can be reduced for all systems if SINR-based power control [44]–[46] is used.

In Fig. 3, the uplink and downlink do not have the same performance for the following reasons:

1) Continuous time-division multiplex (TDM) transmission from radio ports [29] is assumed for all systems. This represents a worst-case interference scenario for the downlink, since all interfering ports are active in all time slots. The uplink traffic, however, is based on an Erlang B model and calls are assigned to the idle time slot with the least uplink interference at each port [27]. The number of servers in each port is determined by the (approximate) number of traffic channels n_c available for each system

$$n_c = \left[\frac{W}{f_s \cdot N}\right] \cdot n_T \tag{6}$$

where $[\cdot]$ indicates the closest integer, W is the total channel bandwidth ($W = 5$ MHz), f_s is the RF channel spacing, N is the reuse factor, and n_T is the number of TDMA channels per carrier. This gives $n_c = 8$ for PACS, $n_c = 30$ for upbanded IS-54, and $n_c = 24$ for DCS-1900. Accordingly, the average time slot occupancy at 1% blocking for each system is: 0.4 for PACS, 0.68 for upbanded IS-54, and 0.64 for DCS-1900. The differences in average time slot occupancy cause the uplink interference environment to be different. (For example, for the same $N = 16$, the uplink performance of PACS is better than that of upbanded IS-54 because of the lower average time slot occupancy.)

2) The user-location specific shadow fading component causes the uplink SIR to have a larger variance than the downlink SIR [see Fig. 5(b)]. On the downlink, all interference signals from different cochannel ports have the same user-location specific shadowing as the desired signal, thus, the downlink SIR is not affected.

From Fig. 3, we can determine the minimum value of $\Lambda(r)$, denoted as $\Lambda(r_{\max})$, that satisfies the SINR requirement of

TABLE II
PORTABLE-TO-PORT LINK BUDGET SUMMARY

	TDMA			CDMA
	PACS	Upbanded IS-54	DCS-1900	IS-95*
Maximum Portable Transmit Power (mW)	400	150	400	50
Combined Antenna Gain G_A (dB)	8	8	8	8
Thermal Noise Power (dBm) (Amplifier Noise Figure = 6 dB)	-114	-124	-115	-101
Required Median SNR at r_{max} $\Lambda(r_{max})$ (dB)	30	30	24	6
Allowed Median Path Loss $L(r_{max})$ (dB)	118	124	125	120
Microcell radius r_{max} (m)	341	464	489	378
Microcell Area (km^2)	0.233	0.431	0.478	0.286

each radio system. For PACS and upbanded IS-54, $\Lambda(r_{\max}) =$ 30 dB seems appropriate for the uplink, and also provides an SINR nearly equal to the 16 dB target SINR on the downlink. For DCS-1900, since the actual SINR performance could be improved further via frequency hopping, we determine $\Lambda(r_{\max})$ such that the SINR is degraded by only 1 dB compared to the maximum SINR achieved at $\Lambda(r) = 40$ dB. This gives $\Lambda(r_{\max}) = 24$ dB for both uplink and downlink.

For a given $\Lambda(r_{\max})$, we can determine $r_{\max}$ using (2) and (3). A link budget calculation example (for the uplink) is shown in Table II, where an average portable transmit power capability of 50 mW is assumed for all systems.[3] The "maximum portable transmit power" shown in the table refers to the average power during the time the signal is on.

Figure 4 shows the uplink performance versus $\Lambda(r)$ for the CDMA IS-95* system. (The uplink is the more critical link in CDMA because it requires accurate power control and does not have code synchronization among users within the same cell to allow orthogonal multiple access [36], as the downlink does.) The performance is given in terms of the maximum offered traffic per microcell that permits $\mathrm{SINR}_{99\%} = -14$ dB. An Erlang B traffic model with 1% blocking is used to generate calls in each microcell. Speech activity is modeled as a binomial process with a 0.5 probability of each call being gated on. SINR-based feedback power control is simulated for all radio links. The simulation is similar to those previously presented [46], [47]. The target SINR threshold is set at -14 dB. The maximum power limit changes with $\Lambda(r)$, which in this case indicates the median SNR at the cell corner assuming the maximum transmit power. For simplicity, no tracking of Rayleigh fading is assumed. The simulations assume perfect Rayleigh averaging in the macroscopic diversity measurements.

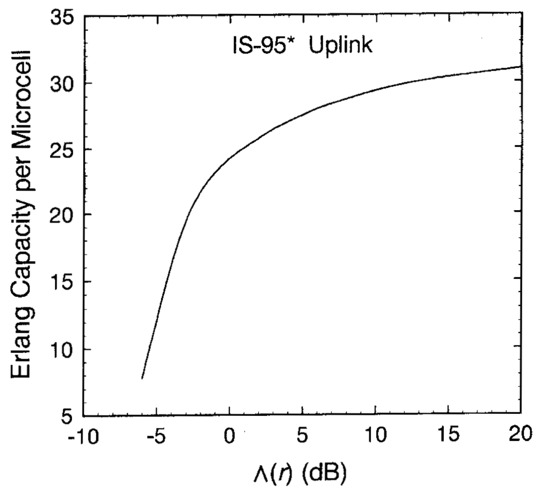

Fig. 4. Erlang capacity per microcell versus median SNR at cell corner $\Lambda(r)$ for IS-95* uplink.

Figure 4 indicates that there is a smooth trade-off between capacity and coverage area size for a CDMA system (this has also been observed in [48]). We choose $\Lambda(r_{\max}) = 6$ dB such that the capacity is reduced by about 10% compared to the maximum achievable capacity at high SNR. The link budget calculation for IS-95* is shown in the rightmost column of Table II.

Note that we consider only thermal noise and noise in the radio receiver amplifiers in Table II. Man-made noise is expected to be small compared to thermal noise in suburban environments at 2 GHz [25]. Noise and distortion in fiber or fiber/coax facilities, e.g., optical receiver noise [49], optical transmitter distortion [49], [50], multipath interference in the

[3] We have deliberately chosen a common basis for uplink average power of 50 mW. This number may be slightly higher than those designated for PACS and upbanded IS-54. Therefore, the actual cell sizes may be even smaller than the results shown here. We estimated that a 3 dB difference in power would translate to at most a 26% reduction in cell size.

optical link [49], cable amplifier noise [51], and ingress noise typical in the upstream cable band (5–30 MHz) of a CATV system, have not been considered and may have some impact on the link budget of the radio system (these noises and distortions can be controlled through careful engineering of the transport facilities). The results in Table II therefore give an upper bound on the coverage area size (see also Footnote 1). It will be shown in the next section that, as the cell size becomes smaller due to possible increased noise or path loss, the resource sharing benefit of simulcasting becomes more significant.

VI. Performance of Simulcast Systems

This section presents detailed simulation analyses of SINR performance and the traffic handling capacity of simulcast systems. We assume that each simulcast group has A contiguous radio ports on a square grid, where A is varied as $A = 1$, 4, 9, and 16. In the simulations, we use the same microcell areas derived in Section V (Table II) for the nonsimulcast case. We will show that, in the simulcast case, the desired coverage is sustained or exceeded under some conditions and degraded under others.

A. Simulcast TDMA

The use of analog transport and simulcasting has several implications on TDMA systems. We first discuss the guard time consideration. In any TDMA radio system, a guard time must be provided in each TDMA slot to prevent uplink signals from overlapping. Since each portable synchronizes its uplink transmission timing to the downlink signal it receives, the guard time for each TDMA slot must be greater than the maximum difference in the round-trip radio propagation delay between any two users served by the same radio port. For example, two users served by a radio port with a coverage radius of 450 m (see Table II) could have a differential round-trip delay up to 3 μs or more. PACS and DCS-1900 provide a guard time of 30 μs in each TDMA slot. Upbanded IS-54 has a guard time exceeding 100 μs.

With a simulcast arrangement, the guard time must also include the difference in round-trip propagation delay over transport cables. The group velocity is 66% of light speed in fiber cable, and 88% of light speed in a typical CATV distribution cable [51]. For a simulcast group consisting of A radio ports on a square grid, the maximum distance between two ports in the same group is equal to $2(r\sqrt{A} - 1)$, where r is the microcell radius. Thus, assuming an arbitrary coaxial cable distribution structure, an additional guard time greater than 20 μs could be required for $A = 9$ and $r = 450$ m. This additional guard time requirement would significantly impact TDMA systems such as PACS and DCS-1900 which have a total guard time of only 30 μs. For these TDMA systems, the transport network architecture must be engineered to minimize differences in cable distance.

Another implication of simulcasting is an increase of delay spread due to differential transport delay. In a distributed antenna system (all ports in a group use the same simulcast air frequency), delay spread caused by the radio channel may increase or decrease with the number of antennas, depending on the propagation environment [11], [13]. However, the distribution cables themselves can cause significant differential delay to the radio signals delivered to and from different radio ports. For example, adjacent radio ports, each having a coverage radius of 450 m, could have a differential transport delay exceeding 2 μs. This will be a serious issue for PACS, since the system does not have equalization and can tolerate multipath with delay spread up to only 1 μs [29]. In order to avoid multipath problems, we assume for PACS that the radio signal is simulcast using a different air frequency in each microcell. This arrangement is similar to a nonsimulcast system except that there is no "network handoff" of calls between different microcells within the same simulcast group. Namely, a user must switch radio frequencies when moving between two microcells in the same group, but the signal is always backhauled over the same cable without need for any switching equipment. Equalization is used in both upbanded IS-54 and DCS-1900, so we consider the use of distributed antennas for these systems.

The use of distributed antennas to improve SIR performance of a TDMA system has been studied in [15]. It was assumed that the size of each radio coverage area is fixed, and as multiple antennas are added to each area the spacing between the antennas decreases. This is different from the simulcast concept considered here where the spacing between radio ports is fixed.

Figure 5 shows log-normal plots of cumulative distributions of SNR and SIR for a TDMA system with a distributed antenna arrangement. These distributions are obtained from simulation similar to results presented in Fig. 3. Simulation parameters for upbanded IS-54 are used: reuse factor $N = 16$, transmit power of 150 mW assumed to be the same for both uplink and downlink, microcell radius of 464 m, average uplink time slot occupancy of 0.68, etc. The distributions of SNR and SIR are not exactly log-normal because of the effect of the distance-dependent path loss. The median uplink SNR decreases as $1/A$, as expected. The variance of the SNR and SIR on both links seems to decrease slightly as A increases, indicating some degree of additional macroscopic diversity improvement. As mentioned earlier, the uplink SIR has a larger variance than the downlink SIR because the user-location specific shadow fading does not affect downlink SIR.

Figure 6 plots $\mathrm{SNR}_{99\%}$, $\mathrm{SIR}_{99\%}$ (from Fig. 5) and $\mathrm{SINR}_{99\%}$ as a function A for simulcast upbanded IS-54. The improvement of $\mathrm{SIR}_{99\%}$ with A has a slope of about 12.5 dB (uplink) and 14 dB (downlink) per decade. This improvement can be explained using a qualitative argument similar to that in [15]. By increasing the number of radio ports per group from one to A, the distance between any two cochannel groups increases by a factor of $\sqrt{A}$. This causes the average strength of each interfering signal to decrease by roughly a factor of $\sqrt{A^{4.5}} = A^{2.25}$, assuming a path loss exponent of 4.5. However, since the number of interfering signals increases by a factor of A in a distributed antenna system, the average power of the total interference is approximately proportional to $A/A^{2.25} = A^{-1.25}$. As a result, the average SIR improves approximately as $10\log(A^{1.25})_{\mathrm{dB}} = 12.5\log A_{\mathrm{dB}}$.

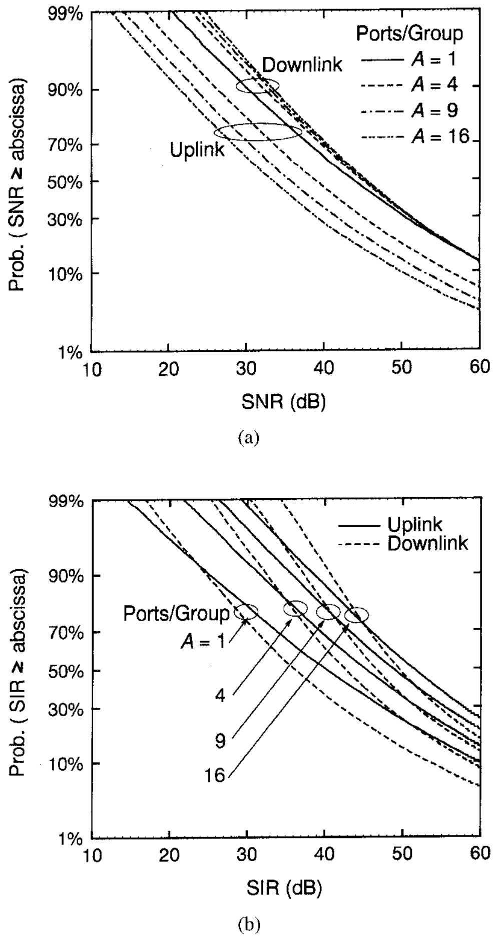

Fig. 5. Cumulative distributions of SNR and SIR for upbanded IS-54 with distributed antennas.

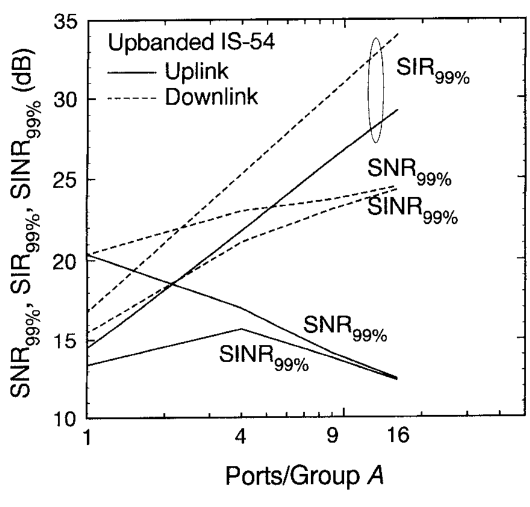

Fig. 6. $\mathrm{SNR}_{99\%}$, $\mathrm{SIR}_{99\%}$, and $\mathrm{SINR}_{99\%}$ as a function of A for simulcast upbanded IS-54.

Despite this significant gain in SIR, the overall system performance is limited largely by multiple antenna noise. As mentioned earlier, the upstream signals from different radio ports in the same group are summed with random phase over the transport network. If the signals are received from A radio ports, the total thermal noise power increases by a factor of A. As a result, the uplink $\mathrm{SINR}_{99\%}$ in Fig. 6 actually decreases by 1 dB for $A = 16$, compared to the result for $A = 1$.

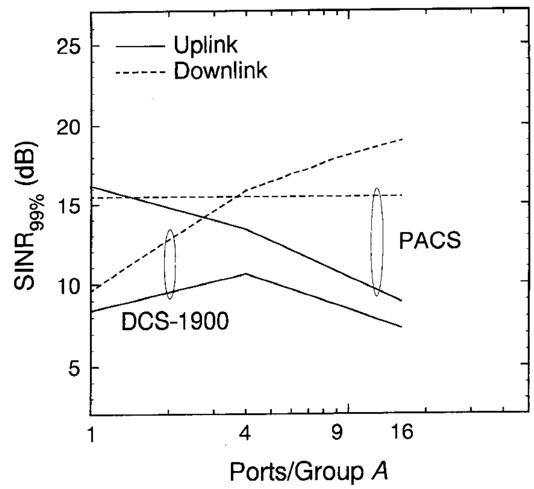

Fig. 7. $\mathrm{SINR}_{99\%}$ as a function of A for simulcast PACS and DCS-1900.

Figure 7 shows $\mathrm{SINR}_{99\%}$ versus A for simulcast PACS and DCS-1900 assuming link budgets for each microcell as shown in Table II. The results for DCS-1900 are similar to those of upbanded IS-54 shown above in that, for both systems, the size of a simulcast group can be increased up to $A = 9$ without degrading the uplink SINR, and up to $A = 16$ with only a 1 dB loss in uplink SINR. PACS represents simulcast TDMA without distributed antennas. For this system, the uplink SINR decreases with A due to multiple antenna noise. The use of distributed antennas is possible in PACS only if the analog transport architecture is designed to keep the differential cable delay between any two ports in a simulcast group below 1 μs.

B. Channel Savings for Simulcast TDMA

We now demonstrate the resource sharing benefit of simulcasting. As one measure of saving, we will compute the reduction in the required number of channels (i.e., call processing circuits) at the central location. A similar method can be used to quantify the saving of other kinds of hardware (e.g., RF circuits). For simplicity, we do not include PACS because the microcell area changes as a function of the group size for this technique.

In a simulcast TDMA system, the number of channels C available in each simulcast group is equal to n_c given in (6): $C = 30$ for upbanded IS-54, and $C = 24$ for DCS-1900. Accordingly, the offered traffic per group at 1% blocking is 20.3 Erlangs for upbanded IS-54, and 15.3 Erlangs for DCS-1900.[4] Given this group traffic capacity, denoted as ρ_G, and given the expected traffic demand per microcell, $\bar{\rho}_\mu$, we can easily determine the average number of radio ports to be assigned to each simulcast group as $\rho_G/\bar{\rho}_\mu$. The equivalent

[4]The actual offered traffic will be slightly less, in general, because of the provisioning of supervisory time slots. In addition, some channel overhead will be required to accommodate handoff traffic [42].

TABLE III
CHANNEL SAVING CALCULATIONS

	TDMA		CDMA
	Upbanded IS-54	DCS-1900	IS-95*
Erlang Capacity/Group ρ_G	20.3	15.3	25.8
Channels/Group C	30	24	37
Average Traffic/Microcell $\bar{\rho}_\mu$ (Erlangs)	3.1	3.4	2.1
Average Number of Ports/Group $\rho_G/\bar{\rho}_\mu$	6.5	4.5	12.3
Average Required Channels/Port $\bar{c}$ (non-simulcast)	8	9	7
Average Required Channels/Group $\bar{C}$ (non-simulcast)	52	40.5	86.1
Channel Saving: $(1 - C/\bar{C})\times 100\%$	42.3	40.1	57

number of channels required in a *non*simulcast system to serve an area of each group is

$$\bar{C} = \frac{\rho_G}{\bar{\rho}_\mu} \cdot \bar{c} \tag{7}$$

where $\bar{c}$ is the number of channels required to support $\bar{\rho}_\mu$ Erlangs of traffic at 1% blocking. Comparing this equivalent number of required channel $\bar{C}$ with C, we can find how much channel saving is achieved through simulcasting. Table III shows an example of channel saving calculation assuming an average suburban traffic density of 7.2 Erlangs/km^2, which is obtained from the following statistics: A typical suburban area in the United States has an average household density of 120 km^{-2} [52], and the average peak-hour telephone usage in a residential household is 0.06 Erlangs [53]. The microcell area sizes given in Table II have been used to determine the values of $\bar{\rho}_\mu$ in Table III. Note that the average numbers of ports per group for both upbanded IS-54 and DCS-1900 are well within the limit $A \leq 9$, where grouping is not limited by multiple antenna noise.

It is clear that the channel saving benefit improves as the size of a microcell becomes smaller such that $\bar{\rho}_\mu$ decreases and $\bar{C}$ increases. We can express $C/\bar{C}$ as

$$\frac{C}{\bar{C}} = \frac{C/\rho_G}{\bar{c}/\bar{\rho}_\mu} = \frac{\eta_\mu}{\eta_G} \tag{8}$$

where $\eta_\mu = \bar{\rho}_\mu/\bar{c}$ is the trunking efficiency of each microcell in a nonsimulcast system, and $\eta_G = \rho_G/C$ is the trunking efficiency of each simulcast group. Thus, $C/\bar{C}$ decreases as the average number of ports per group $\rho_G/\bar{\rho}_\mu$ increases. Fig. 8 shows the relationship between channel saving and $\rho_G/\bar{\rho}_\mu$ for various values of $\bar{\rho}_\mu$. The channel saving improves quite rapidly with $\rho_G/\bar{\rho}_\mu$ for $\rho_G/\bar{\rho}_\mu < 5$, but the improvement quickly saturates regardless of $\bar{\rho}_\mu$. Thus, from the trunking efficiency point of view, there is not much to be gained from increasing the group size beyond $A = 9$. This means that the practical limit on the group size set by multiple antenna

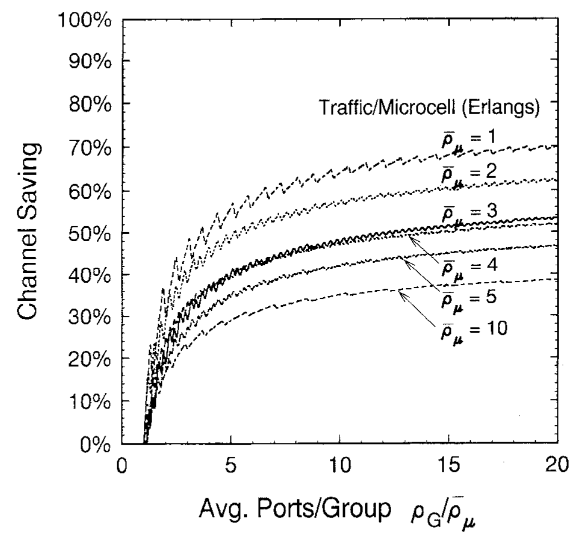

Fig. 8. Channel saving $(1 - C/\bar{C}) \times 100\%$ as a function of the average number of ports per group $\rho_G/\bar{\rho}_\mu$.

noise does not significantly impact the achievable benefit of resource sharing for the TDMA systems. It also indicates that the results in Table III will not significantly improve with an increase in the actual group capacity ρ_G; the values of ρ_G in Table III are conservative estimates in the sense that we did not include the use of SINR power control and the full benefit of slow frequency hopping (for DCS-1900) in the analyses. The channel saving will improve quite substantially, however, if the actual traffic density and/or the size of microcells become smaller. Fig. 8 shows an increase of channel saving by nearly 20% when $\bar{\rho}_\mu$ decreases from $\bar{\rho}_\mu = 3$ to $\bar{\rho}_\mu = 1$.

C. Simulcast CDMA and Channel Savings

In a CDMA system, signals from different multipath components can be resolved and constructively combined by the

RAKE receiver to provide additional diversity against fading. Thus, an increase of delay spread due to differential cable delays in a distributed antenna system can actually improve the radio link quality of each CDMA user [14].

The use of distributed antennas also helps mitigate multiple-access interference. We showed earlier that SIR improves roughly as $12.5 \log A_{\rm dB}$ in a TDMA system because the *effective* distance between cochannel users increases with the group size A. This principle is also valid for a CDMA system except that it applies only to interference from neighboring simulcast groups ("other-group" interference). An even larger amount of uplink interference is produced by users within the same simulcast group ("same-group" interference).[5] These users are power-controlled by the same group server; thus, their relative signal levels are approximately the same at the central location regardless of the use of distributed antennas. As a result, the ratio of signal power to same-group interference power is invariant to the use of distributed antennas.

Even though the use of distributed antennas can only reduce other-cell interference which is the smaller portion of the total uplink interference, the resulting improvement is still significant and is essential in mitigating the impact of multiple antenna noise. Fig. 9 shows the simulated uplink performance of simulcast IS-95*. All the simulation parameters and assumptions are the same as those used in Fig. 4. The link budget considered is such that $\Lambda(r) = 6$ dB for each microcell. Due to multiple antenna noise, the equivalent value of $\Lambda(r)$ is reduced by $10 \log A_{\rm dB}$, yielding $\Lambda(r) = 0$ dB for $A = 4$, $\Lambda(r) = -3.5$ dB for $A = 9$, and $\Lambda(r) = -6$ dB for $A = 16$. Without any reduction of interference by distributed antennas, the performance degradation due to multiple antenna noise would be similar to the limiting effect of $\Lambda(r)$ in Fig. 4. The above reductions in $\Lambda(r)$ would result (see Fig. 4) in a capacity reduction of 14% for $A = 4$, 35% for $A = 9$, and 72% for $A = 16$. Including the benefit of distributed antennas, however, the simulation results in Fig. 9 indicate no reduction in the actual group capacity for $A \le 9$ (the capacity actually increases for $A = 4$), and only an 18% reduction for $A = 16$. This demonstrates the significant benefit of distributed antennas in a simulcast CDMA system.

Although we have not studied the downlink performance of IS-95*, it is evident that the group capacity on this link will improve monotonously with A, given the fact that the downlink does not suffer from multiple antenna noise. In particular, since the system can use synchronized orthogonal codes [36] to minimize same-group interference on the downlink, the reduction of other-group interference by distributed antennas should in this case result in substantial performance improvement. This underscores the validity of our initial assumption that the IS-95* system is uplink limited.

The group traffic demand increases linearly with the group size as shown by the dashed line in Fig. 9. The average Erlang traffic per microcell $\bar{\rho}_\mu = 2.1$ assumed here is determined from the suburban traffic density of 7.2 Erlangs/km^2 (as in

[5]For the suburban propagation model considered in this study, about 70% of the total average uplink interference is produced by same-cell users (assuming no simulcasting). The percentage becomes smaller as median path loss decreases, and the standard deviation of shadow fading increases [54].

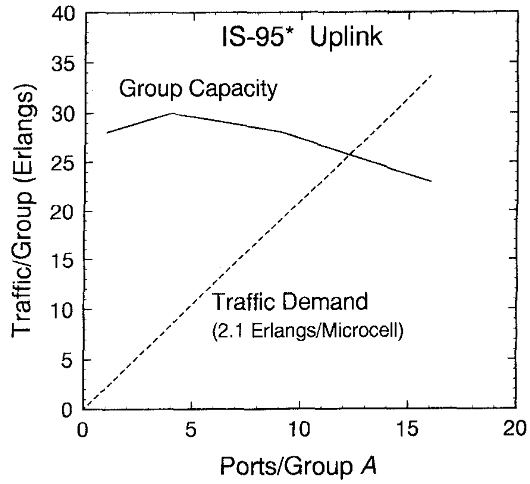

Fig. 9. Erlang capacity per group as a function of A (solid line) for simulcast IS-95* uplink. The dashed line shows traffic demand increasing with A. The point where the two lines cross determines the average group size.

Section VI-B) and the estimated microcell area for IS-95* in Table II. The point where the dashed line crosses the group capacity curve determines the average group size for the simulcast IS-95* system. In this example, the average group size is 12.3, and the group capacity is reduced only by 8% compared to that for $A = 1$. The corresponding channel saving calculation is summarized in Table III. The amount of channel saving for IS-95* is higher than those of upbanded IS-54 and DCS-1900 mainly because its estimated microcell area is smaller. As already noted, the size of microcells has a dominant influence on the resource sharing benefit of a simulcast system.

VII. Conclusion

We have explored the limitations and benefits of simulcasting in suburban microcellular PCS. Among our findings are the following:

- A simulcast system requires the use of distributed antennas to mitigate the impact of multiple antenna noise on the uplink transmission. For TDMA techniques that do not have sufficient delay spread tolerance (e.g., PACS), simulcasting is still possible but an additional link budget margin (a few to several dB according to Fig. 7) must be provided.
- Simulcasting with distributed antennas improves SIR because the *effective* distance between cochannel groups increases with the group size A. As a result, the downlink (no multiple antenna noise) performs better as the group size increases. The simulcast uplink performance is a more complicated function of increasing group size as the SIR increases but the SNR decreases due to multiple antenna noise.
- For simulcast TDMA systems with distributed antennas, a group size of $A = 9$ is a practical (maximum) limit which ensures that simulcasting does not degrade the uplink SINR. This result is based on a contiguous, square group configuration, but it should apply in general because for

a group size as large as $A = 9$, the interference should be dominated by noise and the group size limit no longer depends on the interference conditions (see Fig. 6).

- The group size limit described above is also true for a simulcast CDMA system, given that the group traffic is unchanged. However, a CDMA system can sacrifice traffic handling capacity to accommodate noise if maximizing the group size is the primary system objective.
- From a resource sharing perspective, there is not much to be gained from increasing the group size beyond nine ports. In fact, we have shown that the amount of channel saving stays nearly constant after the group size exceeds five. This means that the practical limit on the group size set by multiple antenna noise does not significantly impact the achievable benefit of resource sharing. A channel saving of 40% to 60% is typical for both TDMA and CDMA systems. This is attributable largely to the sparsity of traffic assumed in suburban environments.
- Considering the implications that simulcasting has on the air interface technique and the transport architecture, CDMA appears to have certain advantages over TDMA. A CDMA system does not have delay spread and guard time constraints as a TDMA system does; such constraints place requirements on the delay characteristics of the transport network. Frequency planning is not required in a CDMA system, but it is a major consideration in the simulcast arrangement for TDMA. CDMA systems employing tight power control will also permit less stringent dynamic range requirements on the associated fiber/coax links [55].
- The computed microcell areas for the suburban propagation model and an assumed portable transmit power of 50 mW average are on the order of 0.2 to 0.5 km^2 (see Table II).

ACKNOWLEDGMENT

The authors would like to acknowledge useful discussions with S. Seidel, J. Foschini, and N. Seshadri.

REFERENCES

[1] FCC, "Amendment of the commission's rules to establish new personal communications services," GEN Docket no. 90-314, Oct. 1993.
[2] L. J. Meyer, "Using fiber optics with analog RF signals," in *Proc. IEEE VTC '89*, San Francisco, CA, May 1989, pp. 398–400.
[3] D. M. Fye, "Design of fiber optic antenna remoting links for cellular radio applications," in *Proc. IEEE VTC '90*, Orlando, FL, May 1990, pp. 622–625.
[4] T.-S. Chu and M. J. Gans, "Fiber optic microcellular radio," *IEEE Trans. Veh. Technol.*, vol. 40, pp. 599–606, Aug. 1991.
[5] K. Morita and H. Ohtsuka, "The new generation of wireless communications based on fiber-radio technologies," *IEICE Trans. Commun.*, vol. E76-B, no. 9, pp. 1061–1068, Sept. 1993.
[6] J. Namiki, M. Shibutani, W. Domon, T. Kanai, and K. Emura, "Optical feeder basic system design for microcellular mobile radio," *IEICE Trans. Commun.*, vol. E76-B, no. 9, pp. 1069–1077, Sept. 1993.
[7] Cablevision Systems Corporation, *FCC Experimental License Progress Reports*, 1992–1993.
[8] Cox Enterprises, *FCC Experimental License Progress Reports*, 1993.
[9] R. W. Donaldson and A. S. Beasley, "Wireless CATV network access for personal communications using simulcasting," *IEEE Trans. Veh. Technol.*, vol. 43, pp. 666–671, Aug. 1994.
[10] N. K. Shankaranarayanan, M. R. Phillips, T. E. Darcie, and S. Ariyavisitakul, "Multiport wireless system using fiber/coax networks for personal communications services (PCS) and subscriber loop applications," in *Proc. IEEE GLOBECOM '95*, Singapore, Nov. 1995.
[11] A. A. M. Saleh, A. J. Rustako, and R. S. Roman, "Distributed antennas for indoor radio communications," *IEEE Trans. Commun.*, vol. 35, pp. 1245–1251, Dec. 1987.
[12] R. A. Valenzuela and L. J. Greenstein, "Performance evaluations for urban line-of-sight microcells at 900 MHz using a multi-ray propagation model," in *Proc. IEEE GLOBECOM '91*, Phoenix, AZ, Dec. 1991, pp. 1947–1952.
[13] P. Hoeher, J. Hagenauer, E. Offer, C. Rapp, and H. Schulze, "Performance of an RCPC-coded OFDM-based digital audio broadcasting (DAB) system," in *Proc. IEEE GLOBECOM '91*, Phoenix, AZ, Dec. 1991, pp. 40–44.
[14] A. J. Viterbi and R. Padovani, "Implications of mobile cellular CDMA," *IEEE Commun. Mag.*, vol. 30, pp. 38–41, Dec. 1992.
[15] K. J. Kerpez and S. Ariyavisitakul, "A radio access system with distributed antennas," in *Proc. IEEE GLOBECOM '94*, San Francisco, CA, Nov.–Dec. 1994, pp. 1696–1700.
[16] P. I. Wells and P. V. Tryon, "The attenuation of UHF radio signals by houses," *IEEE Trans. Veh. Technol.*, vol. 26, pp. 358–362, Nov. 1977.
[17] H. H. Hoffman and D. C. Cox, "Attenuation of 900 MHz radio waves propagating into a metal building," *IEEE Trans. Antennas Propagat.*, vol. AP-30, pp. 808–811, July 1982.
[18] D. C. Cox, R. R. Murray, and A. W. Norris, "800-MHz attenuation measured in and around suburban houses," *AT&T Bell Lab. Tech. J.*, vol. 63, pp. 921–954, July–Aug. 1984.
[19] D. M. J. Devasirvatham, "Time delay spread and signal level measurements of 850 MHz radio waves in building environments," *IEEE Trans. Antennas Propagat.*, vol. AP-34, pp. 1300–1305, Nov. 1986.
[20] A. M. D. Turkmani, J. D. Parsons, and D. G. Lewis, "Radio propagation into buildings at 441, 900, and 1400 MHz," in *Proc. IEE 4th Int. Conf. Mobile Radio Personal Commun.*, Warwick, U.K., Dec. 1987, pp. 129–138.
[21] S. T. S. Chia and A. Baron, "900 MHz attenuation and bit error ratio measurements inside a modern office building," in *Proc. IEE 5th Int. Conf. Mobile Radio Personal Commun.*, Warwick, U.K., Dec. 1989, pp. 33–37.
[22] D. Molkdar, "Review on radio propagation into and within buildings," *IEE Proc.-H*, Feb. 1991, vol. 138, pp. 61–73.
[23] D. M. J. Devasirvatham, R. R. Murray, H. W. Arnold, and D. C. Cox, "Four-frequency CW measurements in residential environments for personal communications," in *Proc. IEEE Int. Symp. Personal, Indoor, Mobile Radio Commun.*, Yokohama, Japan, Sept. 1993.
[24] M. Hata, "Empirical formula for propagation loss in land mobile radio services," *IEEE Trans. Veh. Technol.*, vol. 29, pp. 317–325, Aug. 1980.
[25] W. C. Jakes Jr., Ed., *Microwave Mobile Communications.* Piscataway, NJ: IEEE Press, 1993.
[26] H. W. Arnold, D. C. Cox, and R. R. Murray, "Macroscopic diversity performance measured in the 800-MHz portable radio communications environment," *IEEE Trans. Antennas Propagat.*, vol. 36, pp. 277–280, Feb. 1988.
[27] R. C. Bernhardt, "Time-slot management in digital portable radio systems," *IEEE Trans. Veh. Technol.*, vol. 40, pp. 261–272, Feb. 1991.
[28] H. Sherry, "Progress report on PCS wireless access standards," in *Proc. IEEE NPC '94*, Long Branch, NJ, Mar. 1994.
[29] D. C. Cox, "A radio system proposal for widespread low power tetherless communications," *IEEE Trans. Commun.*, vol. 39, pp. 324–335, Feb. 1991.
[30] Bellcore Technical Advisories, *Generic Framework Criteria for Universal Digital Personal Communications Systems (PCS)*, FA-NWT-001013, Issue 2, Dec. 1990.
[31] JTC(AIR)/94.02.07-119R3, "PACS ad-hoc TAG base line text (working document)," *T1/TIA Joint Technical Committee on Wireless Access*, June 1994.
[32] C.-E. W. Sundberg and N. Seshadri, "Digital cellular systems for North America," in *Proc. IEEE GLOBECOM '90*, San Diego, CA, Dec. 1990, pp. 533–537.
[33] K. Raith and J. Uddenfeldt, "Capacity of digital cellular TDMA systems," *IEEE Trans. Veh. Technol.*, vol. 40, pp. 323–332, May 1991.
[34] D. J. Goodman, "Second generation wireless information networks," *IEEE Trans. Veh. Technol.*, vol. 40, pp. 366–374, May 1991.
[35] K. S. Gilhousen, I. M. Jacobs, R. Padovani, A. J. Viterbi, L. A. Weaver, and C. E. Wheatley, "On the capacity of a cellular CDMA system," *IEEE Trans. Veh. Technol.*, vol. 40, pp. 303–312, May 1991.
[36] A. J. Viterbi, "The orthogonal-random waveform dichotomy for digital mobile personal communication," *IEEE Personal Commun.*, vol. 1, pp. 18–24, First Quarter, 1994.
[37] JTC(AIR)/94.04.28-022R1, "Proposed CDMA PCS standard," *T1/TIA Joint Technical Committee on Wireless Access*, June 1994.

[38] N. S. Jayant and P. Noll, *Digital Coding of Waveforms.* Englewood Cliffs, NJ: Prentice-Hall, 1984.
[39] D. C. Cox, "Universal digital portable radio communications," *Proc. IEEE*, vol. 75, pp. 436–477, Apr. 1987.
[40] ——, "Co-channel interference considerations in frequency-reuse small-coverage-area radio systems," *IEEE Trans. Commun.*, vol. 30, pp. 135–142, Jan. 1982.
[41] S. Ariyavisitakul and L. F. Chang, "Signal and interference statistics of a CDMA system with feedback power control," *IEEE Trans. Commun.*, vol. 41, pp. 1626–1634, Nov. 1993.
[42] G. J. Foschini, B. Gopinath, and Z. Miljanic, "Channel cost of mobility," *IEEE Trans. Veh. Technol.*, vol. 42, pp. 414–424, Nov. 1993.
[43] P. D. Rasky, G. M. Chiasson, and D. E. Borth, "Hybrid slow frequency-hop/CDMA-TDMA as a solution for high-mobility, wide-area personal communications," in *4th WINLAB Workshop on Third Generation Wireless Information Networks*, East Brunswick, NJ, Oct. 1993, pp. 199–215.
[44] J. Zander, "Performance of optimum transmitter power control in cellular radio systems," *IEEE Trans. Veh. Technol.*, vol. 41, pp. 57–62, Feb. 1992.
[45] G. J. Foschini and Z. Miljanic, "A simple distributed autonomous power control algorithm and its convergence," *IEEE Trans. Veh. Technol.*, vol. 42, pp. 641–646, Nov. 1993.
[46] S. Ariyavisitakul, "Autonomous SIR-based power control for a TDMA radio system," *Int. J. Wireless Inform. Networks*, vol. 1, pp. 187–198, July 1994.
[47] S. Ariyavisitakul, "Signal and interference statistics of a CDMA system with feedback power control—Part II," *IEEE Trans. Commun.*, vol. 42, pp. 597–605, Feb./Mar./Apr. 1994.
[48] V. Erceg and J. F. Whitehead, "Microcell size and architecture analysis from the propagation and capacity points of view," in *Proc. IEEE VTC '94*, Stockholm, Sweden, June 1994, pp. 215–219.
[49] T. E. Darcie and G. E. Bodeep, "Lightwave subcarrier CATV transmission systems," *IEEE Trans. Microwave Theory Tech.*, vol. 38, pp. 524–533, May 1990.
[50] N. J. Frigo, M. R. Phillips, and G. E. Bodeep, "Clipping distortion in lightwave CATV systems: Models, simulations, and measurements," *J. Lightwave Technol.*, vol. 11, pp. 138–146, Jan. 1993.
[51] National Association of Broadcasters, *NAB Engineering Handbook*, 8th ed., Section 4, 1992.
[52] U.S. Bureau of Census, *State and Metropolitan Area Data Book 1991*, U.S. Government Printing Office, 1991.
[53] P. Petersen, "Positioning PCS on the telecom landscape," *Telephony*, p. 27, Dec. 1993.
[54] A. J. Viterbi, A. M. Viterbi and E. Zehavi, "Other-cell interference in cellular power-controlled CDMA," *IEEE Trans. Commun.*, vol. 42, pp. 1501–1504, Feb./Mar./Apr. 1994.
[55] T.-S. Chu and J. F. Whitehead, private communication.

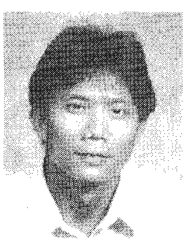

Sirikiat Ariyavisitakul (S'85–M'88–SM'93) received the B.S., M.S., and Ph.D. degrees in electrical engineering from Kyoto University, Kyoto, Japan, in 1983, 1985, and 1988, respectively.

From 1988 to 1994, he was a Member of Technical Staff at Bellcore, Red Bank, NJ, conducting research on wireless communications systems and experimental prototyping of low-power radio links for personal communications. He joined AT&T Bell Laboratories in 1994 and has continued to work in the area of wireless communications. He currently works in the Wireless Communications Research Department of AT&T Research. The topics of his research have included: modulation techniques, equalization, linear power amplifiers, cellular CDMA and power control techniques, coding and frequency hopping, and wireless system architectures and infrastructures. He currently holds eight U.S. patents.

Dr. Ariyavisitakul received the 1988 Niwa Memorial Award in Tokyo, Japan, for outstanding research and publication. He currently serves as Editor for Wireless Techniques and Fading for the IEEE TRANSACTIONS ON COMMUNICATIONS. He is a member of the Institute of Electronics, Information, and Communication Engineers of Japan.

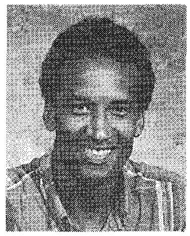

Thomas E. Darcie (SM'94) received the Ph.D degree from the University of Toronto Institute for Aerospace Studies, in 1982.

In 1982, he joined the Technical Staff of AT&T Bell Laboratories, at Crawford Hill, Holmdel, NJ, to study gasdynamics and particle transport in optical fiber fabrication processes. Since 1984, he has investigated the dynamics of semiconductor lasers and amplifiers, subcarrier multiplexing for lightwave systems, and various technologies for coherent systems. He has also studied laser and system requirements for analog lightwave CATV systems and numerous issues related to subscriber local access systems like fiber/coax and passive optical networks. Most recently, he has studied wireless systems for PCS and wireless access. He is presently Director of the Communications Infrastructure Research Laboratory in AT&T Research.

Larry J. Greenstein (M'59–M'67–SM'80–F'87) received the B.S., M.S., and Ph.D. degrees in electrical engineering from the Illinois Institute of Technology in 1958, 1961, and 1967, respectively.

From 1958 to 1970, he worked at IIT Research Institute, primarily in the areas of radio frequency interference and anticlutter airborne radar. He joined AT&T Bell Laboratories in 1970 and has conducted research there in communications satellites, microwave digital radio, lightwave transmission, and wireless communications. He currently heads the Wireless Communications Research Department of AT&T Research. His areas of concentration in the wireless field include measurement-based propagation modeling, microcell system engineering, techniques for diversity and equalization, and methods for estimating and optimizing system capacity and performance. He also co-authored the reprint book *Microwave Digital Radio* (Piscataway, NJ: IEEE Press). He has been a guest editor, senior editor and editorial board member for numerous publications, and has organized and chaired technical sessions for a number of international conferences.

Dr. Greenstein was co-recipient of the IEEE Communications Society's 1984 Leonard G. Abraham Prize Paper Award and the IEEE Vehicular Technology Society's 1993 Neal Shepard Prize Paper Award.

Mary R. Phillips (S'86–M'90), photograph and biography not available at the time of publication.

N. K. Shankaranarayanan (S'83-M'92) was born in India, in 1964. He received the B.Tech degree from the Indian Institute of Technology, Bombay, in 1985, the M.S. degree from Virginia Polytechnic Institute and State University, Blacksburg, VA, in 1987, and the Ph.D degree from Columbia Univeristy, New York, NY, in 1992, all in electrical engineering.

During 1991, he was a visiting researcher at the University of California, Berkeley. He joined AT&T Bell Laboratories, in 1992, and is now with the Broadband Wireless Systems Research Department of AT&T Research. His current research interests cover various aspects of wireless networks, including high-speed packet wireless networks, dynamic capacity allocation, microcellular PCS networks, and radio propagation. His earlier work has been in the areas of WDM optical network architecture and technology, optical beat interference, subcarrier optical networks, and optical fiber sensors.